Refractory Metal Air Vane Leading Edge for Ballistic Missile Defense Interceptor

Archie Ossin *
Martin Marietta Aerospace, Orlando, Fla.
and
Lewis Aronin †
Army Materials and Mechanics Research Center, Watertown, Mass.

A research study has been performed to select, through a combined experimental and analytical effort, a refractory metal material and an air vane leading edge configuration capable of surviving the high-performance advanced ballistic missile defense (BMD) interceptor environments. Five candidate tungsten alloy materials and a tungsten-copper material have been screened for use on the basis of mechanical properties, thermal performance, and resistance to particle impact damage. Only those material fabrication processes which had potential to yield full-scale air vane leading edge hardware were considered. Tensile and coefficient of thermal expansion data were obtained for each material from room temperature to 5000°F. Tests conducted in 5-MW and 50-MW plasma arc facilities evaluated surface recession characteristics over a wide range of pressures and enthalpies. Particle impact damage tests on heated and unheated specimens were conducted in a light gas gun facility using ⅜-in. glass spheres traveling at 10,000 fps. Using the properties obtained, a leading edge design study and thermal stress analysis of several configurations yielded an acceptable design concept which exhibited significantly lower thermal stresses than others considered. The tungsten-hafnium carbide (arc cast) material was the superior candidate in every category.

Introduction

STUDIES conducted by Martin Marietta Aerospace to determine the preferred control method for advanced antiballistic missile systems have consistently shown that air vanes provide the cheapest, lightest, and most reliable system. The quartz-phenolic material which is used as the leading edge material on the SPRINT air vane represents current technology in the area. Analysis shows that this material is not useful for missiles with burnout velocity exceeding 12,000 fps. Beyond this velocity limit, quartz-phenolic leading edge recession is excessive, causing an air vane planform area loss too great for effective missile control. Based on available data, use of a refractory metal leading edge provides the lightest-weight control system over the velocity regime between 12,000 and approximately 15,000 fps.

In this velocity range, the air vane leading edge is subjected to severe thermal, pressure, and particle impact environments. The particle impact environment can be created by natural rain or ice as the missile traverses a hydrometeor cloud, or by solid particles found in the dust and debris cloud from a ground level nuclear burst. Further, the air vane is subject to the particle impact from ablation particles being generated on the missile forebody forward of the air vanes. These particles entrapped in the boundary layer represent a significant design consideration for the advanced interceptor. This problem was addressed for SPRINT, and the air vane design was influenced by this consideration. Finally, the air vane leading edge is affected by secondary particles generated by the impact of either rain or dust on the missile surface forward of the vane. Refractory metals characteristically exhibit high resistance to impact damage and, thus, have potential for protection of the air vane in a particle environment. From these multiple considerations, the emphasis for advanced air vane leading edge design is logically directed toward the development of the refractory metals.

Although emerging transpiration cooling technology is applicable to air vanes and represents an alternative approach to the passive refractory metal system, available information shows that transpiration cooling systems for the velocity ranges discussed will impose a weight penalty over passive systems.[1-3]

Tungsten alloys were selected over other refractory metals, such as molybdenum, columbium, and tantalum, because of their higher strength and higher temperature capabilities. Refractory metals recede more rapidly at temperatures above the melting point than at lower temperatures, where oxidation is the prime cause of recession. Therefore, a high melting point is desirable because it allows the material to oxidize over a wider range of temperature and thereby minimizes surface recession.

Because of the desirable characteristics of tungsten alloys, they have been selected to solve the problem of designing an air vane leading edge for an advanced BMD interceptor.

Technical Approach

The objective of this study was to gain sufficient detailed design information to screen and select the most promising refractory metal materials and to design a flight weight leading edge. The approach taken to meet the objective involved the following steps: 1) Define the missile flight thermal and pressure environment. 2) Survey available materials and select those holding the most promise for air vane application. 3) Measure physical and mechanical material properties, including yield strength, tensile strength, and thermal expansion as a function of temperature. 4) Characterize the thermal recession performance of these materials at representative flight conditions. 5) Evaluate particle impact resistance. 6) Obtain two preliminary baseline air vane leading edge designs with the associated stress field. 7) Select the most promising

Presented as Paper 75-819 at the AIAA/ASME/SAE 16th Structures, Structural Dynamics, and Materials Conference, Denver, Colo. May 27-29, 1975; submitted June 19, 1975; revision received November 24, 1975. This article is based on a study sponsored by the Army Materials and Mechanics Research Center under Contracts DAAG46-73-C-0051 and DAAG46-74-C-0130.

Index categories: Materials, Properties of: LV/M Subsystem Design; Material Ablation.

*Staff Engineer. Member AIAA.
†Materials Engineer.

Table 1 Processing and fabrication of air vane leading edge material candidates

Material	Designation (wt %)	Fabrication	Source
Tungsten-copper	90 W-10 Cu	Powder W → press → sinter → infiltrate with Cu → machine to 1-in. diam bar → machine samples	Sylvania
Thoriated tungsten (powder metallurgy)	W-2 ThO_2	Powder of thoriated W → isostatic cold press to 2 ¾-in diam → machine to 2 ½-in diam → clad with Mo can → seal → extrude 6.5:1 at WPAFB to 0.6×1¼-in. plate → slow cool → remove cladding → machine samples	Westinghouse
Tungsten-hafnium carbide (powder metallurgy)	W-0.35 HfC	Powders of W-HfC → mix → isostatic cold press to 2¾-in diam → machine to 2½-in. diam → clad with Mo can → seal → extrude 6.5:1 at WPAFB to 0.6×1¼-in. plate → slow cool → remove cladding → machine samples	Westinghouse
Tungsten-hafnium carbide (arc cast)	W-0.35 HfC	W rod + Hf foil + C threads → assemble uniformly to electrode → arc melt to 2¾-in diam ingot → machine to 2½-in. diam → clad with TZM can → extrude 6.5:1 at WPAFB to 0.6×1¼-in. plate → slow cool → revove cladding → machine samples	Westinghouse
Tungsten-rhenium-hafnium carbide (powder metallurgy)	W-4 Re-0.35 HfC	Powders of W + Re + HfC → mix → isostatic cold press to 2¾-in. diam → machine to 2½-in. diam → clad with Mo can → seal → extrude 6.5:1 at WPAFB to 0.6×1¼-in. plate → slow cool → remove cladding → machine samples	Westinghouse
Thoriated tungsten (hot isostatic press)	W-2 ThO_2	Powder of thoriated W → isostatic cold press → cut to 0.7×1½x12-in. →presinter → can in Mo sheet → seal → seal → hot isostatic press → remove cladding → machine samples	Westinghouse

Table 2 Density of tungsten alloys

Material	Theoretical density[a] (g/cc)	Measured density (g/cc)	Percent of theoretical density
W-Cu	17.0	17.03	100
W-THO_2 (powder, extrude)	18.9	18.70	99
W-HfC (powder, extrude)	19.3	19.10	99
W-HfC (arc cast, extrude)	19.3	19.12	99
W-Re-HfC (powder, extrude)	19.3	18.89	98
W-ThO_2 (HIP)	18.9	16.90	89

[a]Tungsten theoretical density is 19.3.

air vane leading edge design. 8) Compare the associated stress fields in each design with allowable material strengths.

Five tungsten-alloy materials and one tungsten copper material were selected as candidates for the leading edge materials on the basis of literature reported values of strength at temperature and high melt temperatures. The candidates screened in this program are listed in Table 1.

Material Fabrication

The anticipated material fabrication processes that would be used in the manufacture of full-scale air vane leading edge parts were selected for screening in this study. A summary of the fabrication of each candidate material is shown in Table 1.

Extrusion of the billets was performed in the Wright-Patterson Air Force Base extrusion press at 3200°F. In all cases the billet area reduction was 6.5:1. Extrusions were cooled by placing them in a large container of loose silocel insulation. Four or five hours were required for the extrusion to cool below red heat. This slow cool served as a partial stress relief.

The processing of the thoriated tungsten material by the hot isostatic pressing process (HIP) was not successful in this program. Full densification was never achieved, as evidenced by the data in Table 2. Although the yield was very low, some plasma arc samples were machined. The material was very brittle, and breakage during grinding was very high. Although the HIP process was not successful in this program, the process has potential if used for making air vane leading edges. However, a significant amount of development work would be required.

Detailed fabrication and processing information on the materials used in this program can be found in Refs. 4 and 5.

Mechanical Properties

Tensile Tests

The tensile testing was conducted at Westinghouse Astronuclear Laboratory at a strain rate of 0.5 in./in./min. A high rate of loading was chosen, since the air vane leading edge is subjected to high strain rates in actual flight. All tests on the candidate materials were run on an as fabricated basis.

The tensile values are given in Table 3, and the ultimate strength is plotted versus test temperature in Fig. 1. All candidate materials were brittle at room temperature, showing no elongation. At 1500°F and above, a significant elongation was present among the alloys. The ductile-brittle temperature is between room temperature and 1500°F for the alloy materials. The W-Cu material, however, showed little ductility from room temperature to 2500°F. At 3000°F and above, the W-Cu elongation is much greater.

Table 3 Tensile test values

Material	Test temperature (°F)	Ultimate tensile strength (ksi)	Yield strength (ksi)	Plastic elongation Uniform (%)	Plastic elongation Total (%)
W-Cu	Room	128.0	128.0	0	0
	1500	36.5	33.9	2.1	2.1
	2000	20.2	20.1	0.4	1.0
	2500	16.3	16.0	2.0	3.1
	3000	13.4	12.4	6.0	7.8
	3500	10.7	–	–	–
	4000	9.5	9.3	0.5	11.8
	4500	7.6	7.0	0.8	15.2
	5000	4.0	3.9	1.2	28.2
W-ThO_2 (powder extrude)	Room	94.3	–	0	0
	1500	53.7	33.3	15.1	15.1
	2000	40.3	25.9	8.2	8.2
	2500	31.6	20.0	19.1	29.2
	3000	21.3	12.1	17.8	70.5
	3500	14.1	8.6	2.6	43.2
	4000	9.5	7.1	8.5	49.1
	4500	6.3	5.4	4.3	31.2
	5000	3.8	3.6	1.1	9.1
W-HfC (powder extrude)	Room	92.2	91.2	0	0
	1500	65.4	41.3	24.9	31.8
	2000	71.2	46.2	18.4	29.0
	2500	47.6	37.3	11.3	52.4
	3000	26.2	20.0	8.0	45.3
	3500[a]	–	–	–	–
	4000	9.5	7.0	4.5	39.2
	4500	5.7	4.0	6.3	20.6
	5000	3.5	3.0	3.3	13.0
	3500	15.2	10.6	7.5	84.5
W-HfC (arc melt extrude)	Room	184.8	–	0	0
	1500	103.9	83.8	5.6	8.5
	2000	112.6	97.8	6.2	12.9
	2500	83.9	72.0	3.9	9.9
	3000	66.7	61.5	2.5	9.7
	3500	49.4	46.6	3.2	19.4
	4500	8.6	6.9	8.7	45.1
	5000	4.2	3.3	8.1	69.0
W-Re-HfC (powder extrude)	Room	129.2	–	0	0
	1500	62.9	44.7	7.2	7.2
	2000	49.7	30.0	11.3	11.3
	2500	39.1	29.8	6.1	6.4
	3000	25.2	17.9	0.2	9.0
	3500	17.1	14.2	5.3	19.2
	4000	9.2	8.4	1.3	6.9
	4500	5.5	5.0	4.3	55.4
	5000	4.3	4.0	1.3	8.0

[a] Test invalidated for sample 6 due to fracture out of gage length.

The strength of the W-Cu material is substantially lower than that of the other materials in the 1500-3500°F temperature range. Since copper melts at 1980°F, it does not contribute to the strength of the material in this temperature range. Thus, the material behaves in tension as if it were 80 vol % tungsten. Consequently, the strength is low. At 4500 and 5000°F, the strength of all alloys is so low that no alloy is clearly superior. At room temperature, the measured W-Cu strength is abnormally high; the certification value from SPRINT specification 11181127 is about half the current measurement (Fig. 1). Examination of the sample indicated that the inside tensile cross section appeared to be higher in tungsten content than normal. Whether such a high strength can be explained solely on this basis is not known. Variations in processing variables may be responsible. The thoriated tungsten (PM), is as much as 20,000 psi stronger from 1500 to 3500°F than the W-Cu material. The beneficial strengthening effect of the thoria is evident. However, at room temperature the strength is lower – 90,000 psi as compared to 130,000 psi – for W-Cu.

The W-HfC (PM) material demonstrated a strength peak at 2000°F, which may be attributed to strain aging as a result of the carbon content. This result is not unusual for refractory metals containing carbon, and was found for the arc cast W-HfC alloy as well. This phenomenon, although termed strain aging in the literature, is actually the result of solute interstitial carbon atoms being dragged along with dislocations. Thus, movement of dislocations is more difficult and the strength is raised.[6-7]

This strength peak in the powder metallurgy W-HfC indicates that some HfC was dissolved in the W. The room temperature W-HfC strength is similar to the thoriated tungsten; again, this sample may have been abnormally brittle, lowering its strength. The W-Re-HfC alloy had lower strength from 1500 to 3000°F than the similarly fabricated W-HfC (PM) material. No strength peak was found at 2000°F, as was found for the W-HfC alloys. These results were anticipated, since the carbon level was lowered by the annealing or degassing treatment used on this alloy in processing.

The arc cast and extruded W-HfC alloy had the highest strength of all the alloys at all temperatures. For example, at 2000°F the strength was over 110,000 psi. This is higher than the next closest material by 40,000 psi. At 3000°F, the strength was almost 70,000 psi, which is higher than the next

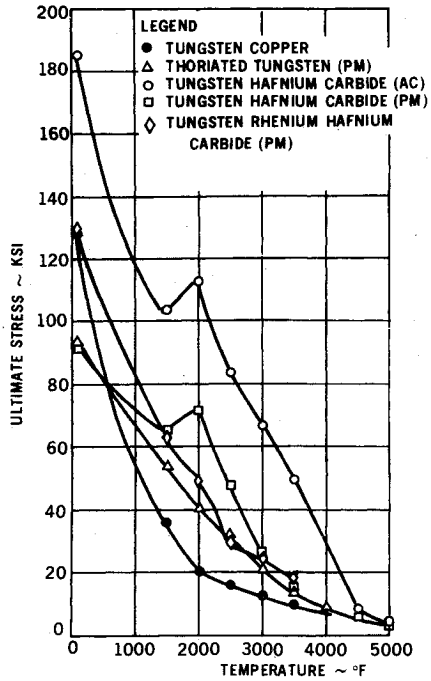

Fig. 1 Ultimate tensile strength of tungsten-alloy materials.

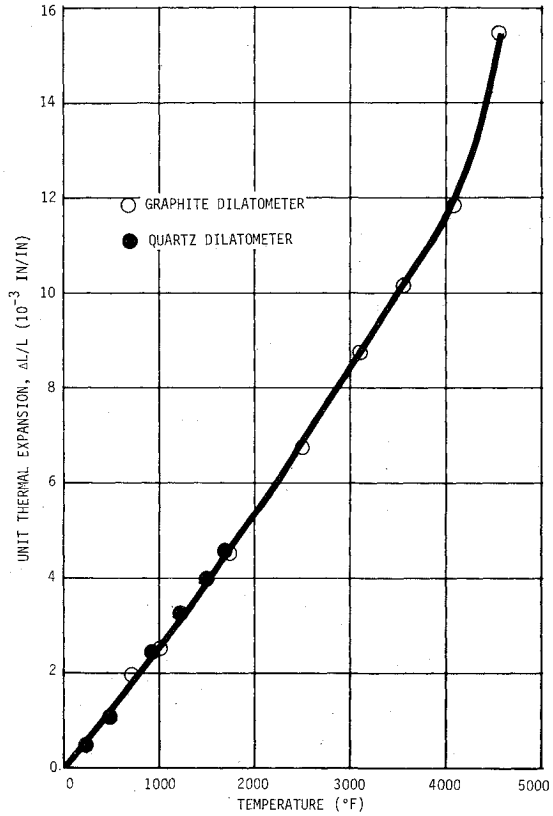

Fig. 2 Thermal expansion of tungsten-hafnium carbide (AC) (W-0.35 wt% HfC).

closest material by 40,000 psi. The HfC is present in such a fine state in this material that effective precipitation hardening has resulted. In principle, the powder metallurgy W-HfC could be heat-treated to the strength level found for the arc cast W-HfC. If, in the future, this could be demonstrated, an air vane could be made more economically of W-HfC by the powder metallurgy and extrusion process, machined or ground to nominal size, solution-treated, final ground, and aged to a high strength level.

Thermal Expansion

Thermal expansion was determined at Southern Research Institute on each specimen by using both quartz and graphite dilatometers. The quartz dilatometer was employed at temperatures up to 1700°F and the graphite dilatometer was used to 4500°F. This provided duplicate data up to 1700°F.

The thermal expansion data are summarized in Table 4. These data were abstracted from thermal expansion curves obtained for each material. The tungsten-hafnium carbide (arc cast) thermal expansion curve (shown in Fig. 2) is typical of the thermal expansion curves obtained for the other tungsten-alloy materials. Values of the coefficient of thermal expansion calculated from this curve and other like curves are given in Table 5 and Fig. 3 for specific temperatures. Table 6 and Fig. 4 present the data in the form of the average coefficient value from room temperature to several elevated temperatures.

Values of thermal expansion were $2.5\text{-}3.0 \times 10^{-6}$/°F for most of the alloys at the lower temperatures. These values are

Table 4 Summary of thermal expansion of tungsten alloys and tungsten-copper

Material (wt %)	Unit thermal expansion (10^{-3} in./in.) 1000°F	2000°F	3000°F	4000°F	Remarks
Tungsten-copper 90 W-10 Cu	3.3	6.4	9.7	10.8	
Thoriated tungsten W-ThO_2	2.4	5.2	8.6	14.4	
Tungsten-hafnium carbide (PM) W-0.35 HfC	2.5	5.3	8.5	12.3	
Tungsten-hafnium carbide (AC) W-0.35 HfC	2.5	5.3	8.4	11.4	
Tungsten-rhenium-hafnium carbide W-4 Re-0.35 HfC	2.3	5.4	9.0	14.5	
Tungsten	2.2	5.1	8.3	11.9	
Copper	9.5	21.7	–	–	Comparative data measured on pure tungsten and pure copper[8]

Table 5 Coefficient of thermal expansion at various temperatures for several tungsten alloys

Alloy	Thermal expansion (10^{-6} in./in./°F)				
	At Room	At 1000°F	At 2000°F	At 3000°F	At 4000°F
W-Cu	3.6	3.4	2.8	4.4	–
W-ThO_2 (PM)	2.6	2.6	3.1	3.6	11.0
W-HfC (PM)	2.6	2.8	3.0	3.4	4.4
W-HfC (AC)	2.5	2.8	3.0	3.1	3.6
W-Re-HfC (PM)	2.3	2.8	3.3	4.0	7.9

Table 6 Average coefficient of thermal expansion from room temperature to indicated temperature

Alloy	Average thermal expansion (10^{-6} in./in./°F)			
	To 1000°F	To 2000°F	To 3000°F	To 4000°F
W-Cu	3.5	3.3	3.3	–
W-ThO_2 (PM)	2.6	2.7	2.9	3.7
W-HfC (PM)	2.7	2.8	2.9	3.1
W-HfC (AC)	2.7	2.8	2.8	2.9
W-Re-HfC (PM)	2.5	2.8	3.1	3.7

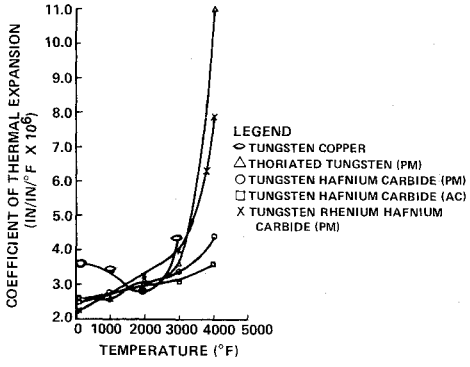

Fig. 3 Coefficient of thermal expansion of several tungsten alloys and tungsten-copper materials.

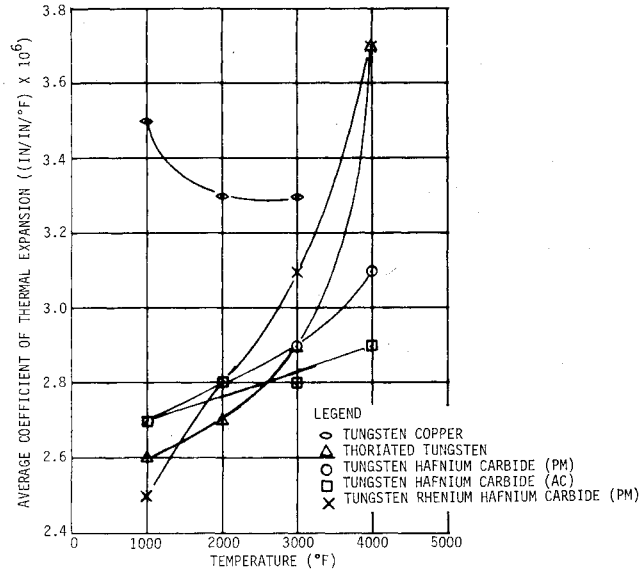

Fig. 4 Average coefficient of thermal expansion of several tungsten alloys and tungsten-copper materials.

not only similar to one another but also to that of pure tungsten. The only significant variation among the materials occurred with the tungsten-copper material, where the expansion was roughly 3.5×10^{-6}/°F. Such a higher value would be anticipated since copper has a much higher expansion than tungsten and tends to contribute to the expansion. At high temperatures, the copper is molten and contributes little or nothing to the expansion. Thus, above 3500°F, the material actually contracted, presumably when the copper was readily exuded from the tungsten. Near 2000°F, an inflection occurred as a result of the initial copper melting.

The W-ThO_2 and the W-Re-HfC alloys had a marked increase in expansion above 3000°F, as shown in Table 5 and Fig. 3. The two W-HfC alloys have the greatest stability and the lowest thermal expansion in the range from room temperature to 4000°F, and at temperatures above 2000°F, the W-HfC (AC) alloy shows slightly less expansion than the W-HfC (PM) material.

Thermal Performance

Recession Performance

The surface recession of a tungsten-based material characteristically falls into two categories, oxidation and melt-phase flow. The surface temperature at which transition from oxidation to melt-phase flow occurs is near the melt temperature of tungsten (6140°F). Because all materials have a significant fall-off in strength near their melt temperature, the effective transition temperature between these two recession regimes is something less than the melt temperature, and must be found experimentally. Knowledge of tungsten performance in both recession regimes is necessary because of the "peaked" profile of a typical advanced interceptor trajectory.

Recession testing was conducted at the 5-MW plasma arc at the Martin Marietta, Denver Division, and the 50-MW plasma arc at Wright-Patterson Air Force Base. The low-pressure 5-MW plasma arc facility was used to define oxidation characteristics of the materials, the temperature at which transition to melt-phase flow occurs, and melt-phase flow in a low-pressure environment. The plasma arc test conditions achieved during the tests are shown in Table 7.

Recession testing was conducted at the 5-MW plasma arc at Martin Marietta, Denver Division, and the 50-MW plasma tungsten-hafnium carbide (arc cast) material. Front look pyrometry data correlated with this recession data yielded the effective temperature at which the transition from oxidation to melt-phase flow occurs. This temperature, which was found to be 5800°F, can be used for all tungsten-based materials at low pressures. Based upon implicit observation at other pressure conditions, this temperature did not vary significantly.

In the oxidation regime, the recession performance among the materials tested was substantially the same (Fig. 6). In the melt-phase flow regime, at low stagnation point pressures (15

Table 7 Denver plasma arc recession test conditions and results

Condition	Cold wall heat flux (Btu/ft^2-s)	Bulk stagnation enthalpy (Btu/lb)	Centerline stagnation enthalpy (Btu/lb)	Stagnation pressure (atm)	Tungsten alloy steady-state recession rate (in./s)	Tungsten copper steady-state recession rate (in./s)	Recession regime
1	5680	3600	4610	6.3	0.169	0.140	Melt phase
2	4370	2950	3820	5.5	0.126	0.050	Melt phase to oxidation transition
3	3650	2240	2750	7.6	0.011	0.011	Oxidation
4	3060	2000	2390	7.2	0.010	0.010	Oxidation

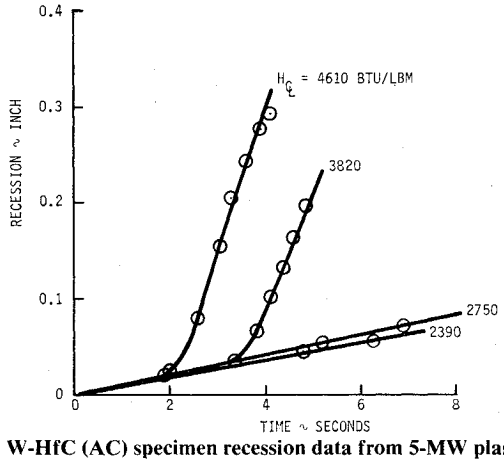

Fig. 5 W-HfC (AC) specimen recession data from 5-MW plasma arc tests.

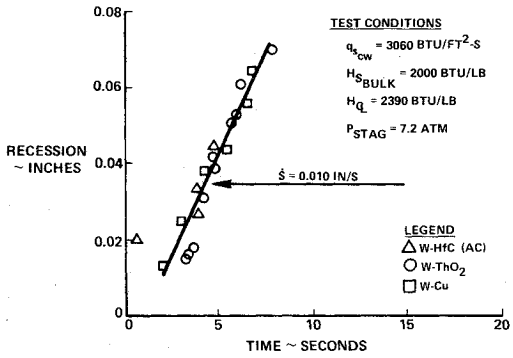

Fig. 6 Tungsten-alloy diffusion limited oxidation recession.

atm and below), the tungsten-copper recession was slightly better than the tungsten alloys. This is believed to be a result of the beneficial effects of copper vaporization. Figure 7 shows an example of this effect from data taken at the 5-MW plasma arc facility. This advantage of the tungsten-copper material found in low-pressure testing was not displayed at the test conditions achieved at the 50-MW plasma arc facility where stagnation pressures were 20-80 atm.

The testing conducted at the 50-MW plasma arc was used to define the effects of high pressure on recession performance over the entire anticipated flight regime. The plasma arc test conditions achieved during the tests are shown in Table 8. A summary of the test data as a function of enthalpy and pressure is shown in Figs. 8-10. It can be seen that the tungsten-hafnium carbide (arc cast) material has superior recession performance over the other materials. The beneficial effects of the infiltrated copper in tungsten-copper, which, at low pressure make this material a good performer, disappear at pressures greater than 15-20 atm. To assess the overall effect of these data on flight performance, the data taken at both facilities have been correlated and incorporated

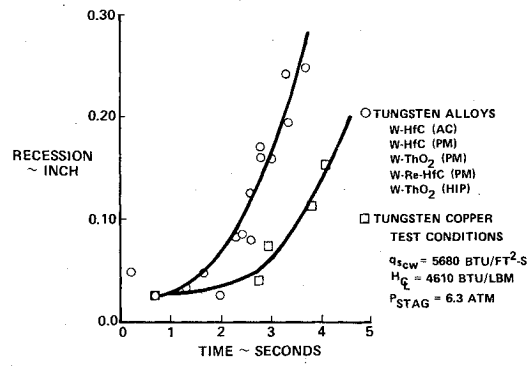

Fig. 7 Low-pressure 5-MW plasma arc data for tungsten-alloy melt phase recession.

into an existing computer code with which flight predictions are made. The performance of W-HfC (AC) and W-Cu as a function of interceptor burnout velocity is shown in Fig. 11. It can be seen that the W-HfC (AC) material is the superior performer in the anticipated advanced interceptor flight environment.

Configuration Design Analysis

The thermal and mechanical property data taken in this program were factored into a thermal stress analysis of several air vane leading edge configurations. A 15,000 fps burnout velocity interceptor trajectory was used as the baseline in this analysis. A Rohm and Haas computer code[9] was used to perform the stress analysis. The time dependent stress field and temperature field at all points in the matrix resulting from the coupled effect of the thermal load and maximum asymmetrical aerodynamic load were computed. Two leading edge design concepts which exhibited significantly lower thermal stresses than others considered are shown in Fig. 12. The configuration providing the lowest stresses was the plug configuration. Figure 13 compares the predicted stresses at the indicated location of peak stress in this con-

Table 8 50-MW plasma arc test conditions

Test point	Centerline enthalpy (Btu/lb)	Stagnation pressure (atm)	Stagnation heat flux (Btu/ft^2-s)
1	5200	83	14650
2	5200	56	12100
3	5200	43	10140
4	5200	23	7420
5	3920	83	10950
6	3920	56	9050
7	3920	43	7580
8	3920	23	5540
9	2200	83	5980
10	2200	56	4940
11	2200	43	4140
12	2200	23	3030

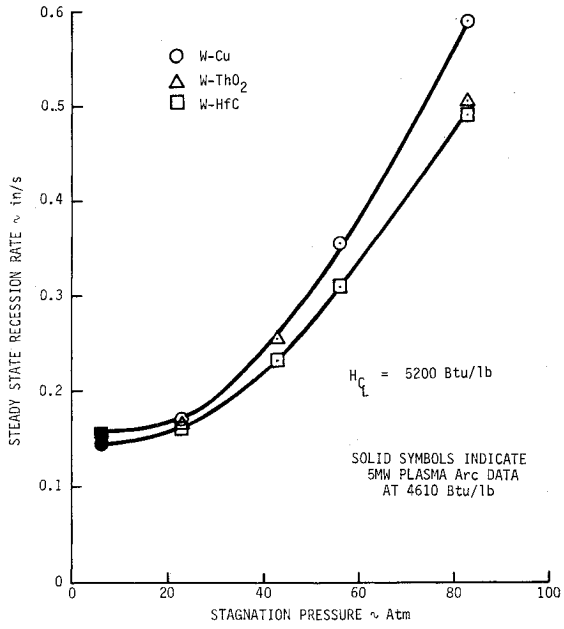

Fig. 8 Steady-state recession rate versus stagnation pressure, $H_{\ell} = 5200$ Btu/lb.

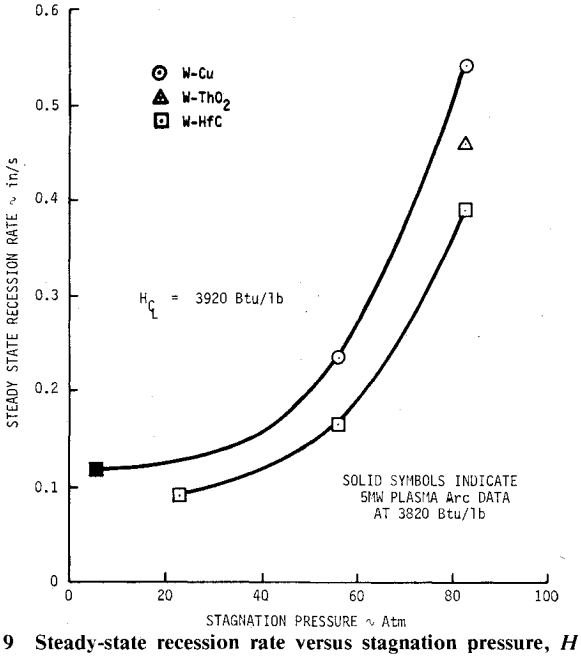

Fig. 9 Steady-state recession rate versus stagnation pressure, $H_{\ell} = 3920$ Btu/lb.

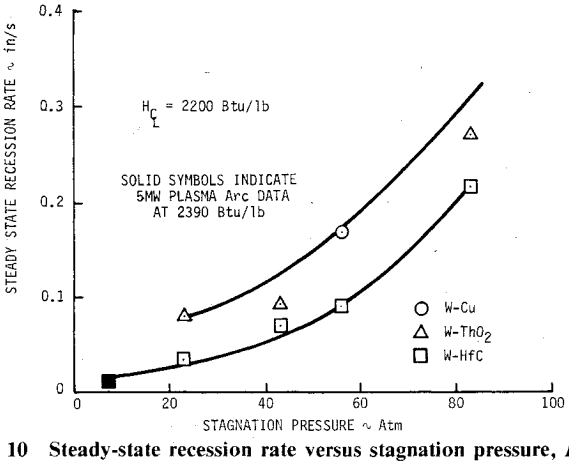

Fig. 10 Steady-state recession rate versus stagnation pressure, $H_{\ell} = 2200$ Btu/lb.

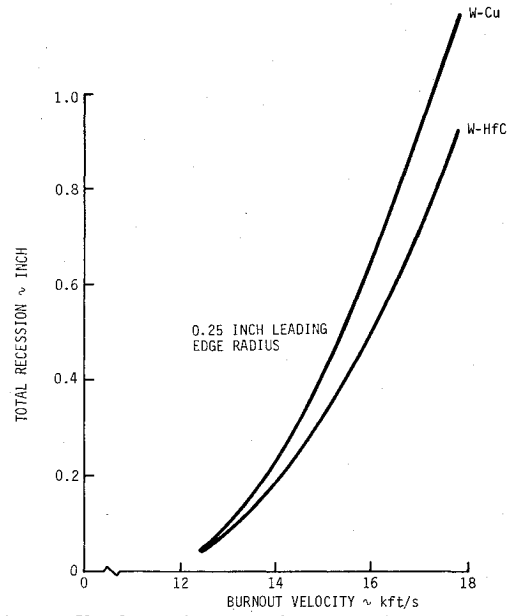

Fig. 11 Total recession versus interceptor burnout velocity.

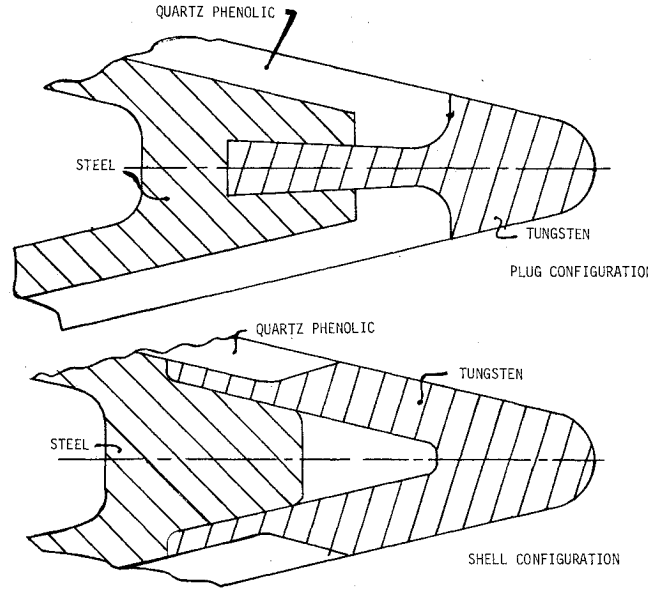

Fig. 12 Refractory vane leading edge concepts.

figuration with material capability. For this figure the temperature at this location can be related to trajectory flight time. The "E" curve shows the predicted values using the elastic modulus. The "S" curve shows the analysis using the secant modulus, and the "A" curve includes consideration of the predicted ablation. The tungsten-hafnium carbide (arc cast) material provides a positive margin in all cases, and is clearly superior to all others considered.

Particle Impact Tests

Large-particle impact tests were conducted on the candidate materials in the Martin Marietta light gas gun, using a ⅜-in. diameter glass ball with an impact velocity of 10,000 fps. The impact angle of 26 deg simulates the anticipated BMD air vane leading edge angle. The testing was conducted at room temperature, 1000, and 4000°F. The test specimens were small rectangular blocks, 2 ⅜-in. long by 1 ⅛ in. wide by ½ in. thick.

In the post-test evaluation and comparison of the relative performance of the candidate materials, consideration was

Table 9 Refractory metal impact performance comparison

Material	Temperature (°F)	M_0/M_i	Structural response			
			Front face cracking	Back face cracking	Side cracking	Edge effects
W-Cu	Room	0.041	Moderate	Moderate	Moderate	Yes
	1000	0.083	Slight	Slight	Slight	Yes
	4000	5.100	None	Moderate	Slight	Partly
W-HfC (AC)	Room	0.031	Extensive	Extensive	Extensive	Yes
	1000	0.024	None	Slight	Slight	Yes
	4130	1.380	None	None	None	No

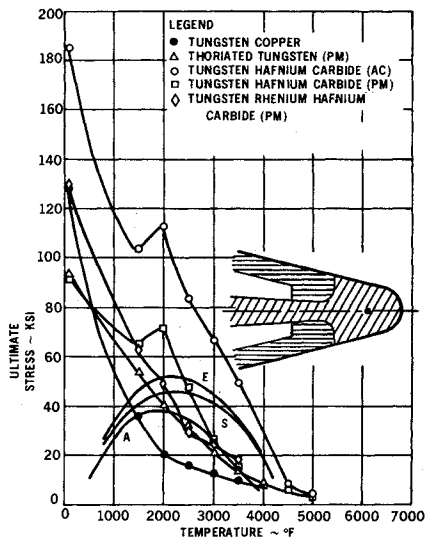

Fig. 13 Comparison of maximum flight stress with material strength – plug configuration.

given to both material cratering and the material structural response. Material cratering was quantitatively determined by crater dimensions and the mass loss ratio. Material structural response was qualitatively determined by the formation, propagation, and the general nature of cracking. Cracking of the specimens ranging from slight to extensive was evident in all of the room-temperature tests and is believed to be attributable to edge effects. The W-Cu material exhibited slightly greater mass loss than the tungsten-alloy material candidates.

The testing at elevated temperature produced a significant increase in the mass loss and associated crater dimensions; however, with the exception of the W-Cu material, virtually no cracking could be attributed to the edge effects. Longitudinal cracks were found inside the W-Re-HfC and W-ThO_2 craters, with hairline cracks penetrating through to the backside of these materials. The impact performance of the W-Cu material at elevated temperature was much inferior to that of the other materials. The poor performance at high temperature is probably associated with the fact that the tungsten matrix has lost much of the copper and presents an 80 vol % dense structure to the impacting particle.

The evidence from this testing shows that the tungsten-alloy materials tested are vastly superior to the tungsten-copper material. This can be seen in Table 9, where W-HfC (AC) performance is compared with W-Cu. In considering the character of the crater and the nature of the cracking, the W-HfC (AC) and W-HfC (PM) appear equal in performance and slightly superior to the W-Re-HfC (PM) and the W-ThO_2 (PM) materials.

Table 10 Summary of program findings

Best configuration	Plug-type design
Material with highest tensile strength at temperature	W-HfC (AC)
Materials with most stable and lowest thermal expansion	W-HfC (AC) W-HfC (PM)
Materials with highest particle impact resistance	W-HfC (AC) W-HfC (PM)
Material which yielded highest positive design margin	W-HfC (AC)
Material with best overall thermal recession characteristics	W-HfC (AC)

Conclusions

The material screening study has yielded a superior candidate from the standpoint of strength, thermal expansion, thermal recession, and particle impact resistance. This is the tungsten-hafnium carbide arc cast material. A leading edge design study and thermal stress analysis of several configurations resulted in the selection of the plug design concept which exhibited significantly lower thermal stresses. This design had more than adequate strength when the W-HfC (AC) material was used. A summary of overall findings of this study is given in Table 10.

References

[1] Kinnaird, L.D., "Controlled Atmosphere Protected Surfaces for Advanced Interceptor Missiles," *Second Aerospace Structures Design Conference*, Sept. 28 and 29, 1970, Seattle, Wash.

[2] Kinnaird, L.D., Cawthon, D.M., and Joyner, C.B., "Active Oxidation Protection for ABM Control Surfaces," AIAA Paper 71-391, Anaheim, Calif., 1971.

[3] Ossin, A. and Cawthon, D.M., "Evaluation of the CONAP Concept for Advanced ABM Nose Tips," Martin Marietta Aerospace, Orlando, Fla., OR 12,486, Feb. 1973.

[4] Hall, R.C., Ossin, A., Aronin, L., Ammon, R.L., and Buckman, R.W. Jr., "Processing and Characterization of Several Tungsten Alloys," *20th National SAMPE Symposium*, San Diego, Calif., April 29-May 1, 1975.

[5] Ammon, R.L. and Buckman, R.W., Jr., "Vacuum Arc Melting of Tungsten-Hafnium-Carbon Alloy," *Journal of Vacuum Science and Technology*, Vol. II, Jan./Feb. 1974, pp. 385-388.

[6] Cottrell, A.H., "Effect of Solute Atoms on the Behavior of Dislocations," *Report of the Bristol Conference on Strength of Solids*, Physical Society, London, 1948, pp. 30-38.

[7] Wilcox, B.A. and Huggins, R.A., "Strain Aging Effects in Columbium due to Hydrogen," *AIME Columbium Metallurgy Symposium, Metallurgical Society Conference*, Bolton Landing, N.Y. June 9-10, 1960 (pub. by Interscience, New York, D.L. Douglas, ed., Vol. 10, 1960, pp. 257-277).

[8] "Thermal Expansion Properties of Aerospace Materials," NASA Tech, Brief 69-10055, July 1969.

[9] Brisbane, J.J., "The Heat Conduction and Stress Analysis of Solid Propellant Rocket Motor Nozzles," Rohm & Haas Co., Huntsville, Ala., Feb. 1969.